

On the relationship between the 500 hPa height fluctuations and the atmosphere thickness over Iran and the Middle East

I. Rousta^{1,2}, M. Doostkamian³, H. Ólafsson⁴, H.R. Ghafarian-Malamiri¹, H. Zhang⁵, A.M. Taherian³, M.O. Sarif⁶, R.D. Gupta⁷ and E.R. Monroy-Vargas⁸

¹Department of Geography, Yazd University, Yazd 8915818411, Iran

²Institute for Atmospheric Sciences, University of Iceland and Icelandic Meteorological Office (IMO), Bustadavegur 7, IS-108 Reykjavik, Iceland

³Department of Geography, University of Zanjan, 3879145371, Iran

⁴Department of Physics, University of Iceland, Institute for Atmospheric Sciences and Icelandic Meteorological Office (IMO), Bustadavegur 7, IS-108 Reykjavik, Iceland

⁵Department of Environmental Science and Engineering, Jiangwan Campus, Fudan University, 2005 Songhu Road, Yangpu District Shanghai 200438, China

⁶Geographic Information System (GIS) Cell, Motilal Nehru National Institute of Technology Allahabad, Prayagraj-211004, India

⁷Civil Engineering Department, Motilal Nehru National Institute of Technology Allahabad, Allahabad-211004, India

⁸Department of Civil Engineering, Universidad Católica de Colombia, Bogotá, Colombia

Received: 15-IV-2018 – Accepted: 5-IX-2018 – **Original version**

Correspondence to: irousta@yazd.ac.ir; zhokzhok@163.com

Abstract

This paper focuses on the relationship between the 500 hPa height fluctuations and the associative atmosphere thickness (AT) over Iran and the Middle East between 1961 and 2013. For this purpose, atmospheric Geopotential Height (HGT) data of the 1000 and the 500 hPa levels were obtained from the NCEP/NCAR database covering the domain of longitudes 25°E to 75°E and latitudes 15°N to 45°N. The correlation coefficient was used to investigate the relationship. The results showed that the daily fluctuations at the 500 hPa height and the AT over the Middle East were low. However, the degree of instability of the AT and the 500 hPa height was higher in the fall season, due to the study region being located in the transition region of different air masses. The lowest instability of the 500 hPa height and the AT was observed in summer due to the dominance of the subtropical dynamical high pressure which was observed in the summer season and in low latitudes of the Middle East. Nevertheless, the greatest effects of HGT on the AT were observed in the middle latitudes. This situation was due to the cold weather which attacked from the high latitudes toward the mid-latitudes, as well as the convection of hot air from the equator to the high latitudes, causing a sharp temperature difference in the middle latitudes and strongly affecting the AT. So, the fluctuations of the 500 hPa reached their maximum in the middle latitudes. In general, there was a significant, direct relationship between oscillations of the 500 hPa height and the AT.

Key words: 500 hPa level, Atmosphere Thickness, Iran and Middle East, fluctuation

1 Introduction

Atmospheric thickness (AT) plays a significant role in atmospheric phenomena. It can be a good guide for estimating precipitation type, front location and many other

phenomena. The AT of the 1000-500 hPa tends to be strongly correlated with the 500 hPa height, so one might expect the patterns in the two fields to be similar and, in fact, they are. Variations of upper-air thickness are related to anomalies in the surface climate. The AT is the vertical



distance in meters from the 1000 to the 500 hPa level. The 1000 to 500 hPa AT is a function of two properties, first, the average temperature of the air between 1000 and 500 hPa and second, the average moisture content of the air between 1000 and 500 hPa. These two properties are combined to produce the virtual temperature. The hydrostatic relation also leads directly to a useful relation describing the AT of the air column between two different pressure levels. The AT is an extremely useful quantity in relating mean-state pressure and temperature anomalies.

A shift to a more meridional atmospheric climate pattern, the Arctic Dipole (AD), over the last decade, has contributed to recent reductions in summer Arctic sea ice extent; the increase in late summer open water area is, in turn, directly contributing to a modification of large scale atmospheric circulation patterns through the additional heat stored in the Arctic Ocean and released to the atmosphere during the fall season (OND). Extensive regions in the Arctic, during late fall beginning in 2002, had surface air temperature anomalies of greater than 3°C and temperature anomalies above 850 hPa of 1°C. These temperatures contribute to an increase in the 1000–500 hPa AT field in every recent year with reduced sea ice cover. The AT of the atmosphere between the two constant pressure levels has a direct correlation with the average temperature, therefore, in areas where the air column is warmer than the surrounding areas, the AT is more than that. The AT variations are caused by the advection of external air masses, dynamic ridge/trough of air, and heating/cooling on the Earth’s surface.

AT maps correspond to temperature maps; therefore, a closed low height region involves a cold air pool and a closed region with a high height is a package of hot air. The arrangement of iso-thickness contours, as well as the topography of the iso-pressure levels play an important role in the creation and direction of synoptic system temperatures. With the fall of cold air, the air mass becomes denser (i.e. its density goes up) and, subsequently, the atmosphere becomes thicker. On the contrary, with the fall of hot air, the air mass is expanded (hence, its density decreases) and molecules tend to diverge, which results in the increase of the AT.

Reduction in the AT due to cooling is different, but with an average of about a 1°C decrease in atmosphere temperature, accompanied by 66.5 m decrease in the AT (Alijani, 2006). Studying contours with similar AT can reveal areas where cold/hot air or tongues of cold/hot air are concentrated (Farajzadeh Asl et al., 2009; Ghaemi, 2007; Zarrin et al., 2010).

Studying the AT at a global level is not a new field. For example, in 1976, Blackmon (1976) measured the 500-hPa height in the northern hemisphere. In 1982, Rogers and Van Loon (1982) examined the anomalies of the sea and the 500-hPa levels in the northern hemisphere. In 1996, Houghton (1996) studied the orbital fluctuations of the 500-hPa heights in short, medium and long-term scales. But, in Iran this issue was not very noticeable and was

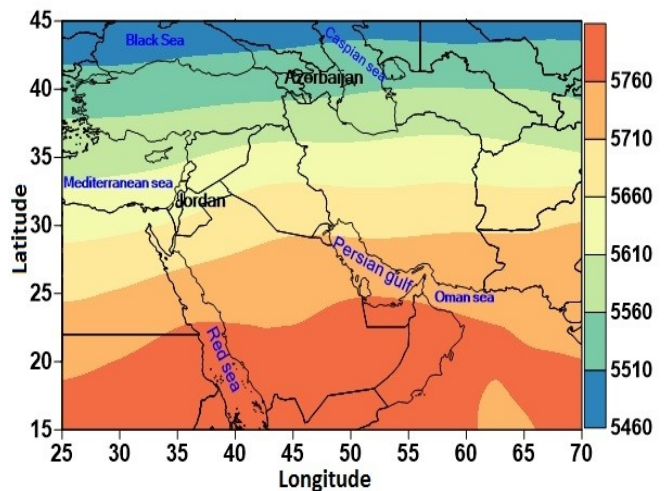


Figure 1: The study region and the mean of the AT (m) during the study period (1961-2013).

not studied very much. For example, Rousta et al. (2016) investigated the AT Pattern of Iran’s Pervasive Frosts and showed that pervasive frosts occur alongside contours that have a thickness of 5300 to 5400 geopotential meters. In fact, pervasive frosts occur alongside these contours that are as thick as the atmosphere (especially the ones that are 5300 geopotential meters thick). And in most studies, this issue has been addressed in the form of other, superficial studies. For example, in studies about extreme temperature and precipitation, or in studies about atmospheric blocking (Azizi et al., 2015a,b; Iman et al., 2014; Rousta, 2016), severe cold, or flash floods.

Most of the Middle East, especially Iran, has experienced heavy droughts and heatwaves, as well as an increase in temperatures in recent years. The values of the AT are regressing with an increase in the temperature. The AT can be a good guide for estimating precipitation type, front locations, and many other phenomena. Based on what was mentioned, few studies have focused on the relationship between the AT and the 500 hPa height fluctuations over Iran and the Middle East. There are a limited number of publications focusing on the relation between them. The study of AT patterns as one of the important tools for identifying and managing natural hazards plays a significant role in preventing economic and human losses. Therefore, this study sought to examine the relationship between the AT and the HGT (the 500 hPa height) fluctuations in Iran and the Middle East.

2 Materials and methods

2.1 Materials

In this study, the HGT atmosphere data of the 1000 and 500 hPa levels, which covers the domain of longitudes

25°E to 75°E and latitudes 15°N to 45°N and spans the statistical period between 1961 and 2013, were used as the major data source. This data set was obtained from National Centers for Environmental Prediction/National Center for Atmospheric Research (NCEP/NCAR), and the spatial resolution of these data was 2.5x2.5 angular degrees (Fig. 1).

2.2 Methods

The hydrostatic relation leads directly to a useful relation describing the thickness $Z_0 - Z_1$, of the air column between two pressure levels, P_0 and P . Using the ideal gas law to eliminate density, the thickness is found to be (Eq. 1):

$$Z_0 - Z_1 = \frac{RT}{g} \ln \frac{P_0}{P} \quad (1)$$

where Z_0 and P_0 are respectively, the height and pressure at the reference level or the level just below the studied layer. T is the mean temperature of the layer.

Given that the AT between these two layers (500 and 1000 hPa) is representative of the state of all layers, after extracting atmospheric data, the AT between the 1000 and 500 hPa was calculated, using the hypsometric equation (Eq. 2):

$$Thickness = HGT_{500} - HGT_{1000} \quad (2)$$

Then, to gain an overall picture of the AT, descriptive features (central profiles, profiles of distribution, dispersion profiles) of the AT and HGT for each month were investigated. In order to analyze the atmospheric patterns and their effects on AT fluctuations, the pattern of each month was identified and analyzed by using principal component analysis (PCA).

The purpose of PCA is to obtain structures, via a new set of variables that most closely and efficiently represent an original data set of N observations on M interconnected variables. In other words, to simplify the data set for purposes of interpretation and understanding. The new variables are orthogonal to one another and therefore uncorrelated.

A matrix of covariances (or correlations) is set up from the M original variables ($M \times M$). The first new variable (first PC), or Empirical Orthogonal Function (EOF) which contains the largest proportion of the total variance in the data set is extracted (by computer routine). It represents a linear function of the M variables of the form (Eq. 3):

$$z_i = a_{i1}x_1 + a_{i2}x_2 + \dots + a_{iM}x_M \quad (3)$$

where $a_{11}, a_{12}, \dots, a_{1M}$ are the partial coefficients. This set of coefficients (also called loadings or weights) $a_{11}, a_{12}, \dots, a_{1M}$ in the first principal component comprises the first eigenvector. $EOF1$ represents an "average" variable for the ($M \times M$) matrix. The second PC ($EOF2$) is orthogonal to the first and extracts the largest proportion of the remaining variance, and so on.

The principal component (or EOF_i) can be expressed as shown in Eq. 4:

$$z_i = a_{i1}x_1 + a_{i2}x_2 + \dots + a_{iM}x_M \quad (4)$$

where $i = 1, 2, \dots, M$.

The correlations between EOF_i and the M variables are called the component loadings, and the square of the loadings is the proportion of associated variance.

Then, the Correlation Coefficient was used in order to investigate the relationship between the AT and HGT for each month. Using this method, the degree of variability of the AT was analyzed over time using Regression analysis which is a statistical technique for analyzing and modeling the relationship between variables (Harrell, 2015). The regression model is used to describe the variability of the dependent variable (y) by the change of the independent variable (x). In time analysis, the simplest definition of the process of climate change is expressed by linear regression. In this regard, the best line must be determined. Therefore, this line exists on the coordinates of the points derived from the two variables x and y .

The correlation coefficient with a value of 1 means a perfect positive correlation and the value $r = -1$ means a perfect negative correlation. In the regression, if the β sign is positive, r is positive and if the β sign is negative, r is negative.

3 Results and discussion

3.1 Spatial characteristics of the monthly 500 hPa iso-height contours

The computation of the monthly spatial distribution of mean and coefficient of variations of the 500 hPa and the AT layer in winter (JFM) indicates that the average of the 500 hPa iso-height was 5676.1 m in January, 5674.4 m in February and 5701.2 m in March (Table 1). Thus, the AT layer (Table 2) followed the 500-hPa contours (5522.3 m in January, 5534 m in February and 5579.3 m in March). This suggests that whenever the 500-hPa iso-height contour increased, the AT layer of the Middle East atmosphere also increased. Due to the proximity of the central profiles, it can be said that almost throughout the winter, the form of monthly average distribution of the 500 hPa iso-height AT layer is nearly normally distributed, and that there is a fairly large harmony and uniformity between them (Table 1, 2). In February, it was more impressive, since variance and standard deviation are the relatively appropriate and widely used indicators for analyzing the distribution of dispersion; this index increases with the influence of various and dissimilar air masses, while decreasing with the diversion of different air masses. The highest standard deviation and the variance of the 500-hPa iso-height contours and the AT corresponded to February and the lowest amount

Table 1: Spatial characteristics of the monthly 500 hPa iso-height contours of Iran in the 1961-2013 period.

Parameter	Winter				Spring	
	Jan	Feb	Mar	Apr	May	Jun
Mean	5676.1	5674.4	5701.2	5749.2	5798.5	5829.2
Median	5677.8	5675.6	5699.6	5749.6	5801.5	5831.5
Mode	5633.5	5633.5	5660.7	5698.2	5748.3	5839.1
Variance	397.5	414.9	400.8	334.8	201.8	160.0
SD*	19.9	20.4	20.0	18.3	14.2	12.6
CV*	0.35	0.36	0.35	0.31	0.24	0.21

Table 2: Same as Table 1 but for the AT.

Parameter	Winter				Spring	
	Jan	Feb	Mar	Apr	May	Jun
Mean	5522.3	5534.1	5579.3	5649.5	5715.6	5773.5
Median	5523.7	5533.0	5577.9	5650.0	5716.5	5773.5
Mode	5471.5	5480.1	5544.8	5613.2	5690.0	5751.2
Variance	405.5	511.8	371.8	211.6	128.9	83.5
SD*	20.1	22.6	19.3	14.5	11.4	9.1
CV*	0.36	0.40	0.34	0.25	0.19	0.15

*SD and CV denote standard deviation and coefficient of variation, respectively.

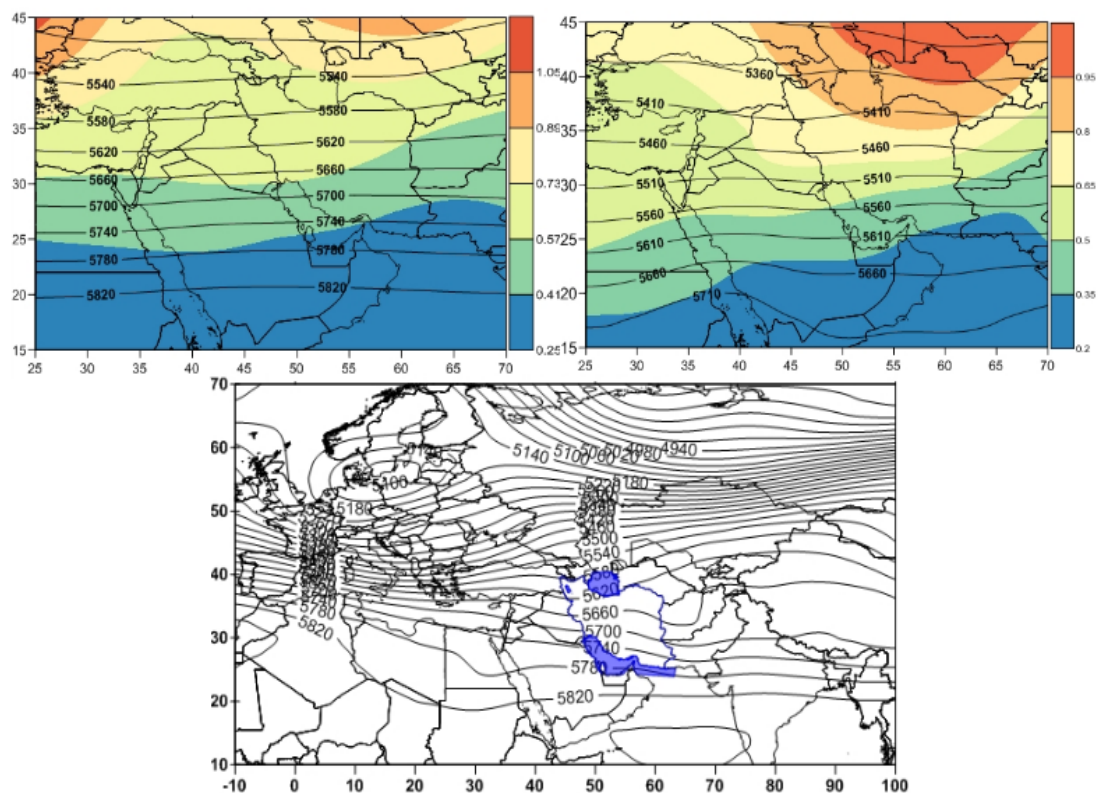


Figure 2: Spatial distribution of monthly mean of CV and representative day in January for the 500 hPa HGT and AT in the 1961-2013 period.

respectively occurred in January and March. The largest coefficient of variation of the 500 hPa iso-height contours and the AT layer of the Middle East in February (0.36 and 0.40), and the smallest coefficient of variation in January

(0.35 and 0.36) is observed (Table 1 and 2). The low CV represents stability and order in climate variability and fluctuations, and high CV indicates instability. Therefore, it can be said that changes in the 500 hPa iso-height contours

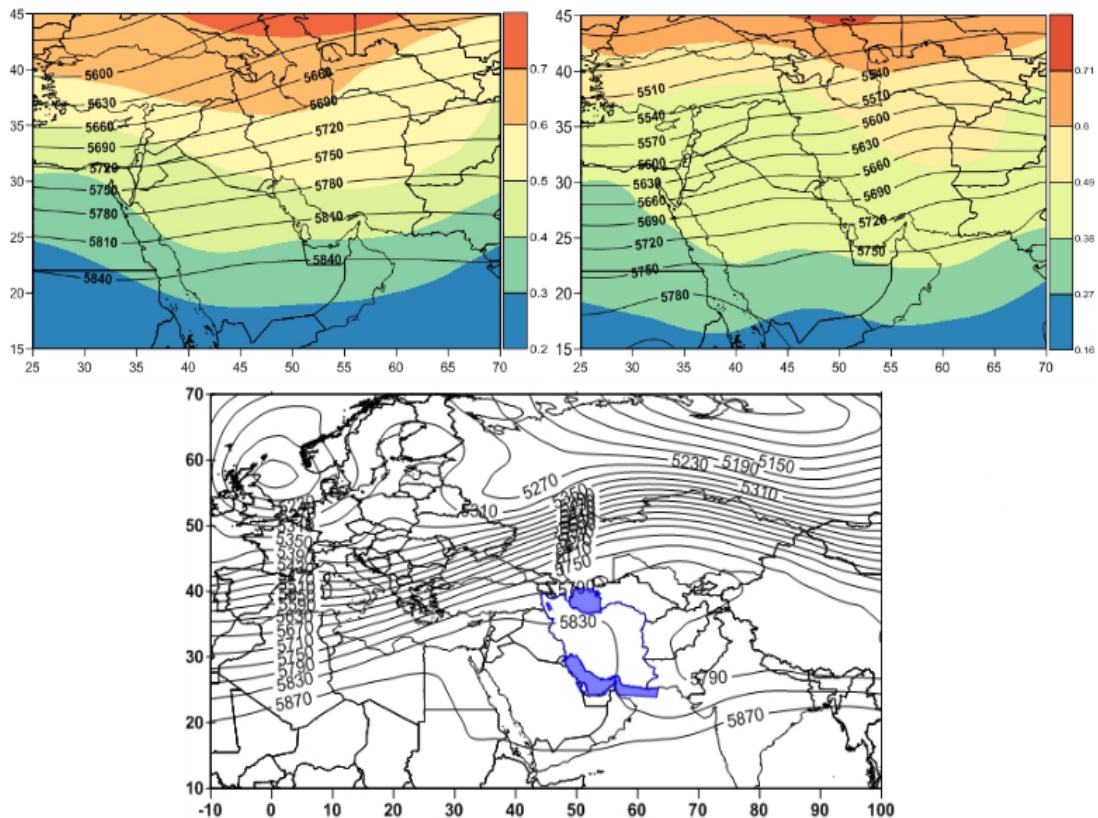


Figure 3: Same as Fig. 2 but for April.

and the AT layer in the Middle East have high order and stability in the winter season (Table 1, 2).

Spatial distribution of mean and CV of the 500 hPa and AT indicate that the minimum CV of the 500 hPa and AT was in the south of Saudi Arabia (0.2 in January), and the maximum CV was in the northwest of Turkey, also in January (0.79) (Fig. 2). This situation may be due to the fact that in low latitudes, especially near the Equator, both coefficients of variation present lower fluctuations because air masses hardly change over the year. While toward higher latitudes and in the middle latitudes, due to the influence of cold weather from northern latitudes and the penetration of hot air mass from lower latitudes, there is a sharp difference in temperature (Fig. 2). This affects the fluctuations in the 500 hPa and AT, as in these latitudes there is the highest coefficient of variation and the lowest amount of the AT. In order to carry out the synoptic analysis of atmospheric patterns and effects of fluctuations of the 500 hPa on the AT, the representative day of the 500 hPa height of one month for each season is presented in Fig. 2. As can be seen in January, the deployment of omega-shape iso-height in northern Europe caused the southward deviation of flows and subsequent influx of cold weather from Europe and the Mediterranean Sea into the Middle East and affected the weather in the whole of the region (Fig. 2).

As in winter, the analysis of the CV of the 500 hPa

iso-height contours and the AT is presented in Fig. 3 for spring. The figure shows that the maximum coefficient of variation of the 500 hPa iso-height contours and the AT in the Middle East region occurred in April. Therefore, maximum coefficient of variation of the 500 hPa iso-height contours were in the northern half of Turkey (0.6) and its maximum value in the AT observed in the east and north east of Iran (0.46). In order to carry out the synoptic analysis of the atmospheric patterns and the effects of fluctuations of the 500 hPa on the AT, the representative day of the month of April for the spring season is presented in Fig. 3.

As seen from the Fig. 3, a wave of winds from the North Atlantic with a height gradient of 450 m crossed the northern and central parts of the Middle East and the northern parts of the Caspian Sea due to the presence and progress of an iso-height system in the central and northern regions of Russia which created a ridge with height gradient equal to 500 meters. Thus, in the northern regions of the Middle East, there is an orbital flow, and because of the rapid flow of various types of air masses, fluctuations in the AT are very high. However, the southern regions have experienced calm and stable conditions owing to their remoteness from the range of deployment of these air masses. Therefore, the south latitudes of the Middle East have the least fluctuations and changes in AT. The northern Atlantic currents in May, as in April, enter the northern regions of Africa and Western

Table 3: Monthly spatial characteristics of the 500 hPa HGT in Iran and the Middle East in the 1961-2013 period.

Parameter	Summer				Fall	
	Jul	Aug	Sep	Oct	Nov	Dec
Mean	5845.2	5850.0	5833.7	5801.6	5753.4	5710.3
Median	5846.5	5853.5	5837.4	5803.4	5751.9	5708.8
Mode	5816.6	5820.4	5837.4	5770.7	5732.5	5675.9
Variance	204.8	200.5	208.1	171.8	229.3	371.6
SD*	14.3	14.2	14.4	13.1	15.1	19.3
CV*	0.24	0.24	0.24	0.22	0.26	0.33

Table 4: Same as Table 3 but for the AT.

Parameter	Summer				Fall	
	Jul	Aug	Sep	Oct	Nov	Dec
Mean	5804.4	5797.6	5746.6	5677.1	5607.5	5554.2
Median	5805.5	5797.3	5748.0	5676.7	5606.6	5553.4
Mode	5785.0	5766.8	5722.5	5656.4	5578.1	5513.1
Variance	87.0	102.2	92.6	123.0	204.7	348.0
SD*	9.3	10.1	9.6	11.1	14.3	18.7
CV*	0.16	0.17	0.16	0.19	0.25	0.33

*SD and CV denote standard deviation and coefficient of variation, respectively.

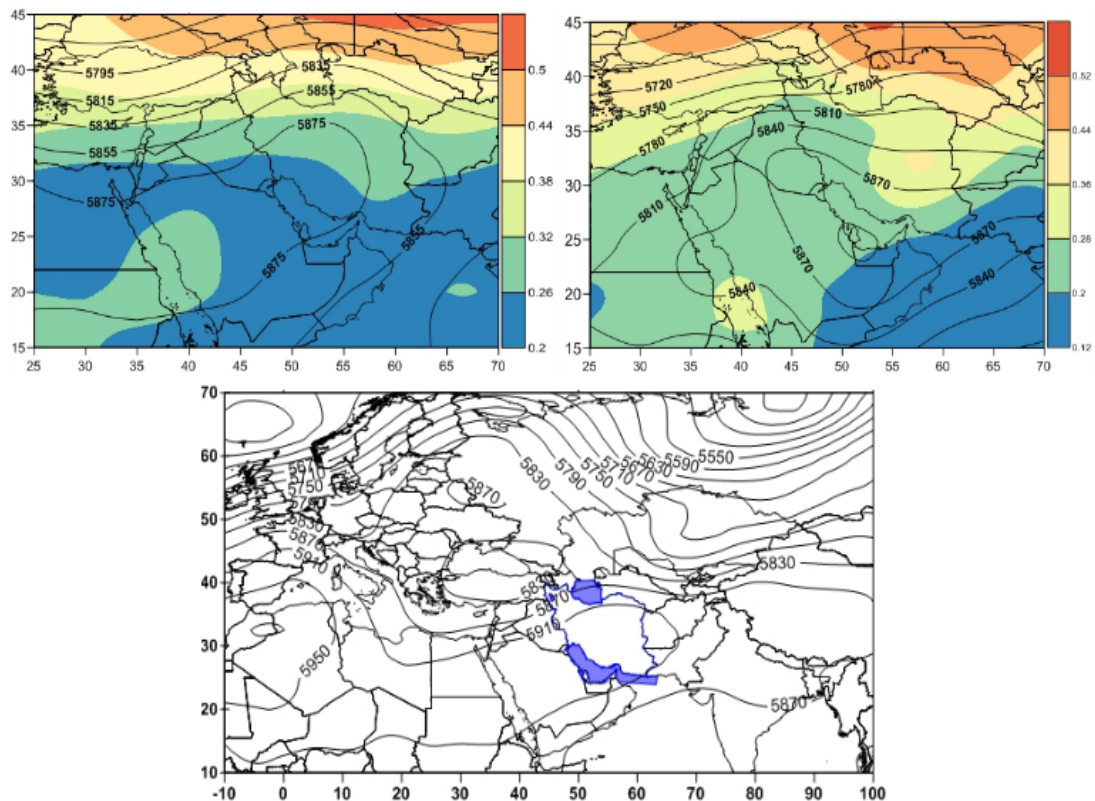


Figure 4: Spatial distribution of monthly mean of CV and representative day in July for the 500 hPa HGT and AT in the 1961-2013 period.

Europe, while the two low-height systems in the northern Mediterranean and eastern parts of Turkey are blocked the air streams, causing their diversion toward the southern latitudes and fluxing the cold weather to Middle East regions

(not shown). These high-density and cold air masses caused the atmospheric depression and reduced the AT in the northern parts of the Middle East (see Fig. 3).

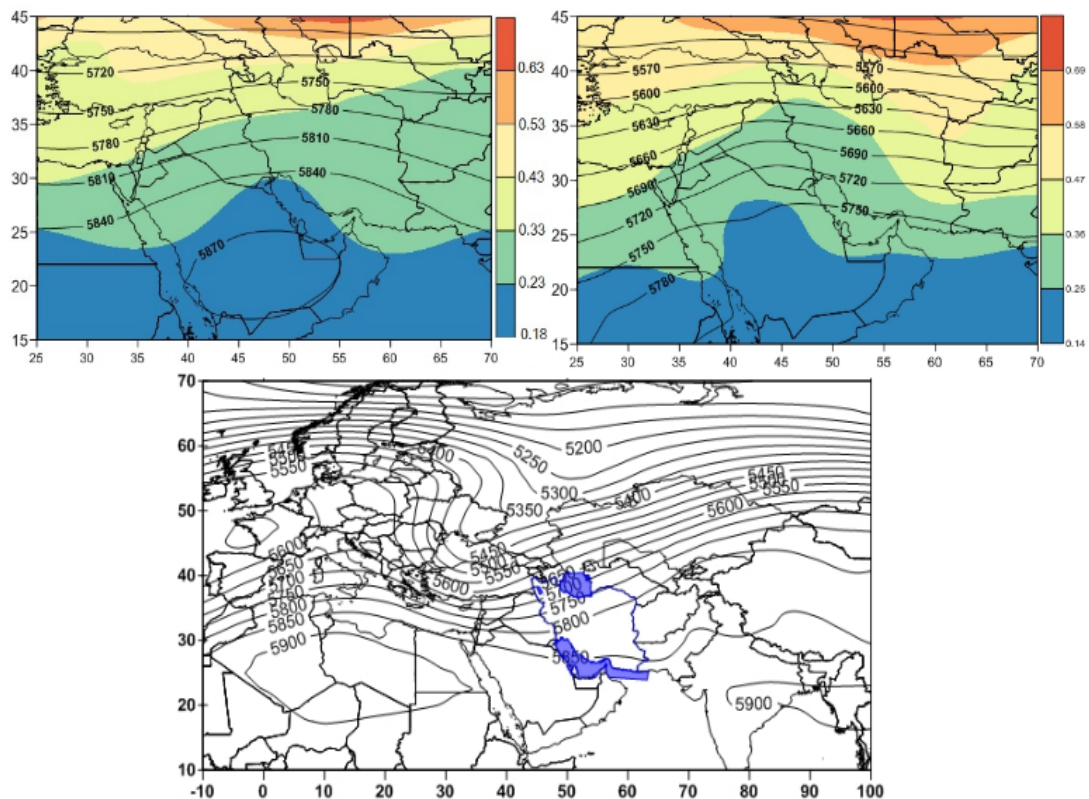


Figure 5: Same as Fig. 4 but for October.

The monthly average of coefficients of variations of the 500 hPa iso-height contours and the AT in the summer season (JAS) indicates that the average of the 500 hPa iso-height contours in July were 5845.1 m; in August, 5849.9 m; and in September it was 5833.7 m (Table 3). The average of the AT in July was 5804.4 m; in August 5797.5 m and in September 5746.6 m, so that there was the maximum average of the 500 hPa iso-height contours and the AT in summer (Table 4). During the warmest period of the year, northern and northeastern parts of Africa, most of Saudi Arabia and many parts of Iran were under the dominance of the Azores subtropical high-pressure and created very severe sustainability conditions. This condition was such that it banned the stream of Western winds and low-pressure systems to the Middle East. The insignificant fluctuations of the 500 hPa iso-height contours and the AT by comparing the central profiles, indicate that there is a large harmony and uniformity between them. This means that decreasing or increasing the 500 hPa iso-height contours contributes to decreasing or increasing changes in the AT. The highest level of change in the 500 hPa iso-height contours was in August, 56.72 m (5872.16 and 5820.43), and the lowest was in July 51.66 m (5868.28 and 5816.61) and the highest range of changes in AT in the summer was in August 54.33 m (5821.11 and 5766.77), and the lowest was in July 38.15 m (5823.14 and 5784.99) (Table 3 and 4).

Considering that the monthly values of central profiles and the 500 hPa iso-height contours are close to each other, it could be said that nearly all summer the shape of the distribution of the 500 hPa iso-height contours and the AT is close to the normal distribution, and it has a high level of harmony in the summer (Fig. 4).

In order to investigate more precisely, the condition of the 500 hPa iso-height contours and the AT, the average of CV of the 500 hPa iso-height contours and the AT are presented. Fig. 4 shows that the lowest coefficient of variation of the 500 hPa iso-height contours is a value of 0.2 in the summer, observed in Saudi Arabia, the Persian Gulf, southern Iraq and the Arabian Sea, and in the case of the AT, it can be observed in southern regions of Saudi Arabia, Oman and the Arabian Sea. And the highest fluctuation rate of the 500 hPa iso-height contours is 0.44 to 0.47 in the northern parts of Turkey and 0.42 in the north east of Iran and northern Turkey. The 500 hPa iso-height contours in the Middle East in July show that the Azores sub-tropical high pressure (STHP) has been dragged into southern Europe and over France (in meridian motion) and covered the Middle East region (in orbital motion). As the main core of this high-pressure at the 500 hPa level was in the central and southern regions of Iran and parts of the Persian Gulf (Bahrain, UAE, Qatar) (Fig. 4 Table 3).

In summer, the Azores STHP is located over Iran, and its central core with about 5900 geopotential meters is deployed over the Red Sea, eastern regions of Saudi Arabia, and North Africa. In addition to the establishment of the core of the Azores STHP in July, a wave of winds from the North Atlantic, after its penetration into Western Europe and parts of the Mediterranean Sea led to create a less deep trough with a height gradient of 60 m in the middle regions of the Mediterranean Sea. But since the Azores STHP is in the Middle East region, these winds were diverted to higher latitudes, passing through the northern regions of Iran (Fig. 4). The spatial distribution map of mean of coefficient of variation of the 500 hPa iso-height and the AT in fall season indicate that the mean of the 500 hPa iso-height in October was 5801.5 m in November, 5753.4 m and in December it was 5710.3 m (Table 3). And the average of the AT in October was 5677 m; in November, 5607.5 m; and 5554.2 m in December (Table 4). The average of the 500 hPa iso-height and the AT during the fall season significantly decreased, so that the average of the 500 hPa iso-height rose up to 90 m and the AT dropped (122 m), respectively.

This situation shows that the AT is heavily influenced by the 500 hPa iso-height contours, but the reduction of the 500 hPa iso-height contours and the AT in the northern and southern regions of the study area are not the same, and at higher latitudes it was greater than at lower latitudes. A vertical drop in the pressure in the hot air layer is slower and more intense in the cold air layer. Therefore, in the southern regions of the Middle East, due to the presence of hot air layers, the AT increased, but in the northern regions, due to a decrease in the average temperature, the AT decreased. Fig. 5 shows that the lowest coefficient of variation of the 500 hPa iso-height contours in October in the range of 0.18 to 0.32 and in the AT from 0.14 to 0.25, covered most of the Middle East region and toward the higher latitudes, the magnitude of the coefficient of variation increased. The southern regions of the Middle East are still affected by the Azores STHP, while the northern regions are placed in the path of higher latitude air masses and experienced higher and stronger fluctuations than southern regions.

Fig. 5 shows atmospheric patterns and the effects of fluctuations of the 500 hPa on the AT for a representative day of October for the fall. The northern Atlantic streams entered the Mediterranean Sea from the northern regions of Africa, so that in the western and central parts of the region, a ridge with a gradient height of 200 meters was created, and the northern parts of the Middle East are located in front of its trough. Therefore, the upper convergence was accompanied by cold weather advection, and on the other hand, the winds of the Icelandic low-pressure crossed the central regions of Europe, in the western part of the Black Sea there was a negative vorticity, causing the cold weather to settle on the Black Sea. Both of these streams merged in the northwest of Iran, Azerbaijan and Turkey and crossed the northern regions of the Middle East. The largest phenomenon of the 500 hPa level in the southern Middle East is the deployment

of the Azores STHP in North Africa that extends up to the central parts of Saudi Arabia. The highest AT was in the same areas of North Africa and the central parts of Middle East (5900 meters).

3.2 The correlation coefficient of the 500 hPa iso-height contours and the AT on the Middle East

The correlation coefficient of the 500 hPa iso-height contours and the AT on the Middle East (Fig. 6) shows that in winter there is strong correlation with the Middle East climate, especially in the southern regions of Middle East. The highest correlation coefficient was 0.93 in the southern regions of Iran in March and the lowest correlation coefficient in the northern regions of Turkey was 0.70 in January. In the spring, the 500 hPa iso-height contours and AT show a strong correlation with the atmosphere of the Middle East, especially in its southern regions. The maximum correlation coefficient in the spring was in April and ranged from 0.9 to 0.94, located in the regions of Saudi Arabia, the Persian Gulf, the southern and central parts of Iran, and in May in the western regions of Iran (0.9) and it was 0.84 in southern regions of Saudi Arabia in June. In this way, fluctuations of the 500 hPa iso-height contours are directly related to the AT in the Middle East region. It is characterized by a negligible coefficient of variation of 500 hPa levels and AT, which indicate that the AT has not changed significantly during the statistical period. It should be noted that the correlation coefficient of the 500 hPa iso-height contours and AT of the Middle East at the beginning of spring (April) has the highest correlation coefficient and at the end of spring (June), has the lowest correlation coefficient. This situation may be due to the fact that in winter, the 500-hPa level with cold air transfer from the higher latitudes AT of the Middle East had a heavy influence. While in the spring, due to the retraction of the Westerlies to higher latitudes, the fluctuations in the AT declined.

In summer, the 500 hPa iso-height contours and the AT show strong correlation with the atmosphere of the Middle East, especially in the western regions of Turkey and southwest of Saudi Arabia, from 0.82 to 0.85 in July and August (Fig. 7). The highest correlation coefficient in the whole summer season was 0.98 in September in the western regions of Turkey and the lowest correlation coefficient was 0.54 in July; there are low values too, from 0.62 to 0.68 in September and August, in the northeastern part of Iran. Consequently, the 500 hPa iso-height contours have the highest correlation coefficient with iso-thickness contours compared to the other seasons of the year. This is because the Middle East atmosphere during the summer season, contrary to other seasons of the year, is influenced by the Azores STHP, but in other seasons of the year there is a penetration of different air masses from different latitudes and polar regions.

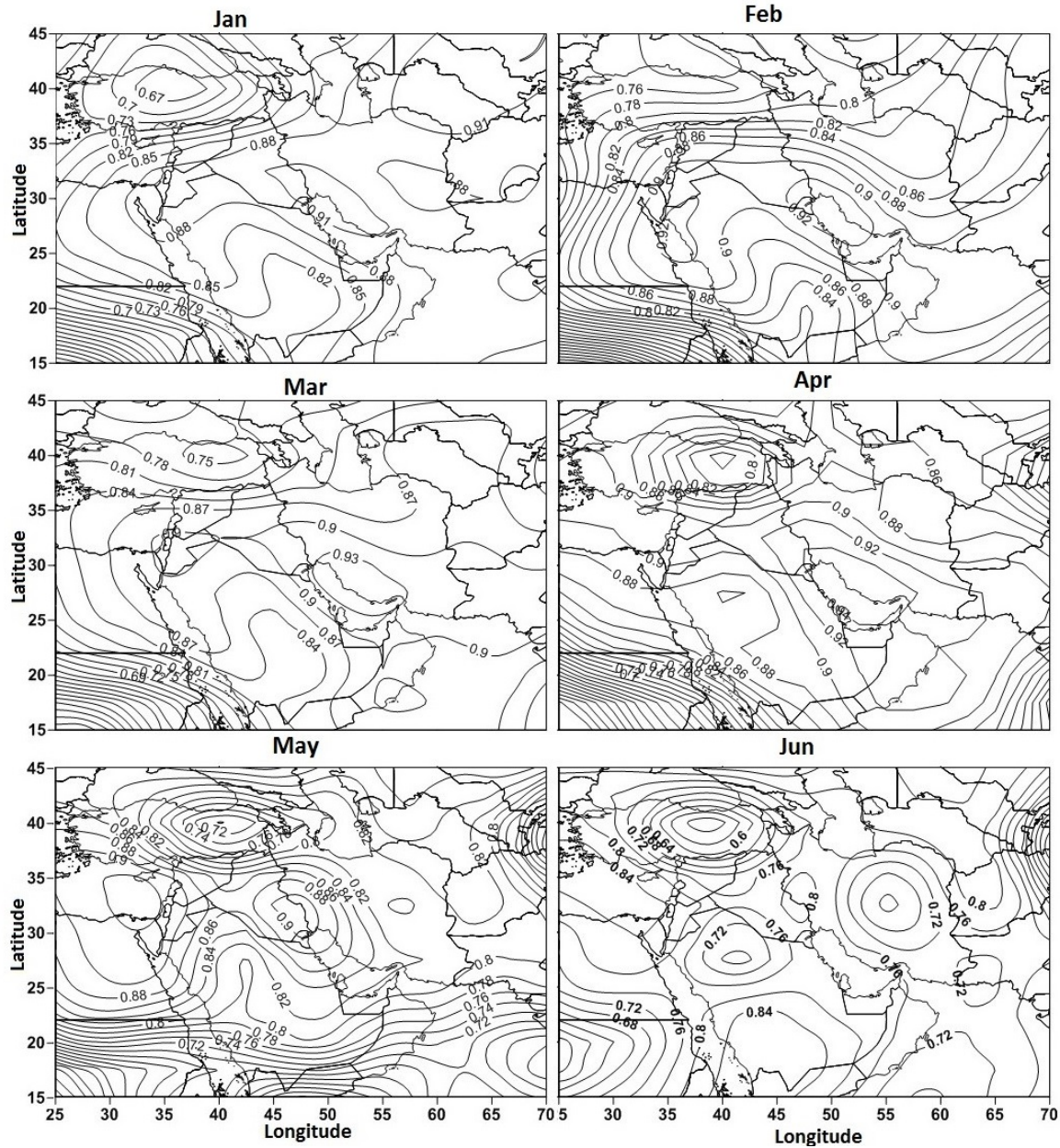


Figure 6: Spatial distribution of correlation coefficient of the 500 hPa HGT and the AT for the winter and spring seasons over the Middle East in the 1961-2013 period.

The AT over the Middle East in the fall (Fig. 7) has a high correlation with its 500 hPa iso-height contours, with a maximum correlation of 0.94 in November; 0.84 in October and 0.93 in December. The highest correlation coefficient of the 500 hPa iso-height contours and the AT were in the Persian Gulf region, eastern Saudi Arabia and southwestern regions of Iran in November (0.94), and the lowest correlation coefficient was in the central regions of Turkey and central regions of Iran in December (0.63-0.75).

Therefore, the AT in the study area has a very strong correlation with the geopotential height of 500 hPa, which varies considerably in different seasons and places (Fig. 2,

3, 4, 5). The high correlation coefficient in the winter in the Persian Gulf regions is likely due to the influx of air masses and sudden currents from the high latitudes, and these air masses can penetrate to the area only if they are strong. In summer, the highest correlation coefficient is found in the northern regions of the Middle East (in Turkey) and the lowest in the southern and eastern regions. This is probably due to the influx of different currents of high latitude in winter season and the continuous and constant presence of the Azores STHP in the summer season, and in the spring and fall due to the development and retraction of different air masses in different latitudes of the Middle East (Fig. 6, 7).

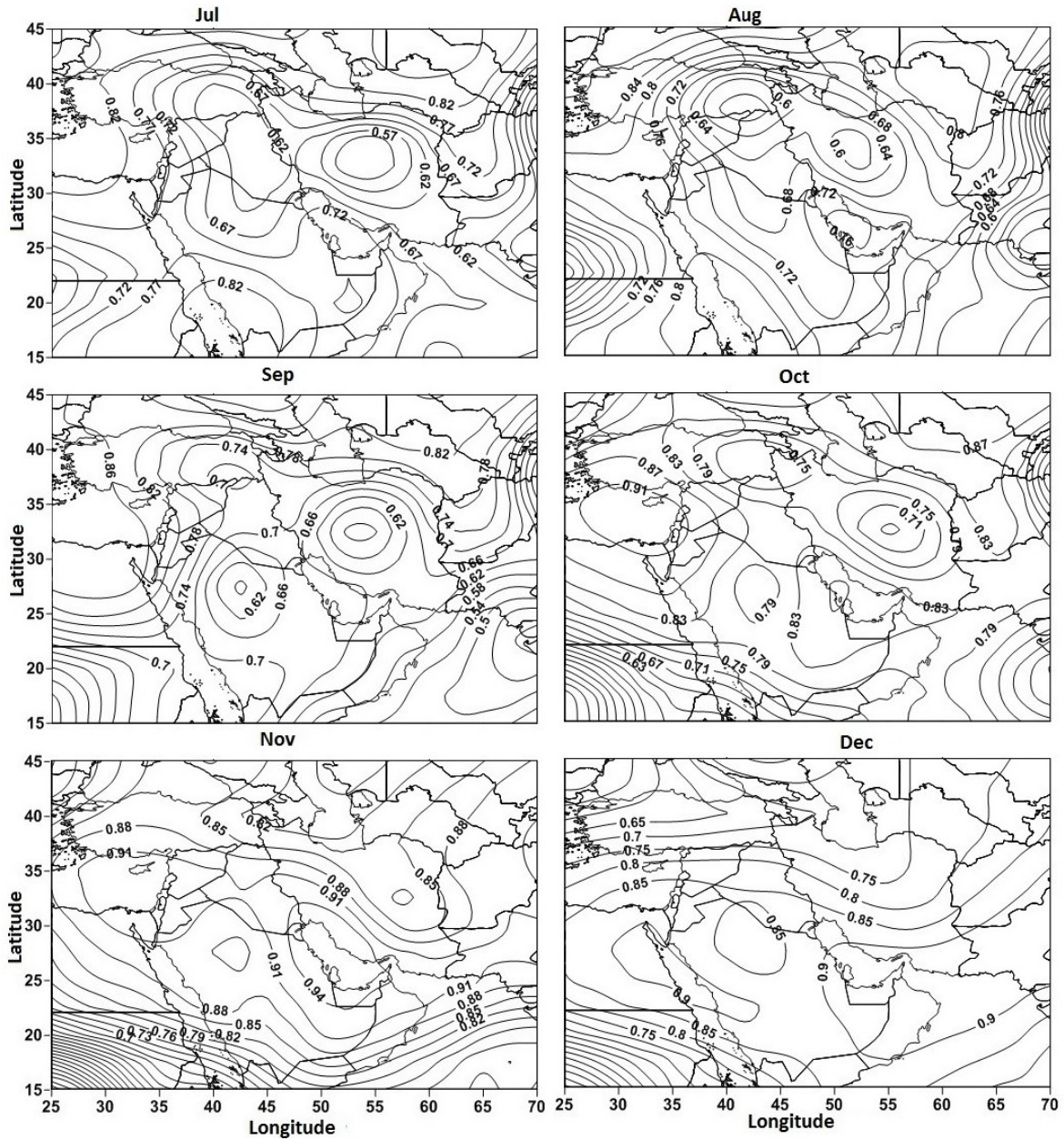


Figure 7: Spatial distribution of correlation coefficient of the 500 hPa HGT and the AT for the summer and fall seasons over the Middle East in the 1961-2013 period.

4 Conclusion

The purpose of this paper is to analyze the fluctuations of the 500 hPa height and their association with the AT over Iran and the Middle East. For this purpose, HGT atmosphere data from the 1000 and 500 hPa levels was obtained from NCEP/NCAR database covering the domain of longitudes 25°E to 75°E and latitudes 15°N to 45°N.

The results showed that the atmosphere of the study area in the winter season has the lowest AT. Because in this season, the area is affected by high latitude currents, especially the Mediterranean trough and the influx of cold weather from Europe. This information is consistent with result of the research done by Rousta et al. (2018b). The

fluctuation of the AT of the Middle East from January to February and March is very low, because, during winter, it is not affected by different air masses, and therefore has a lot of stability, and there are few fluctuations. The Arctic warming trend in the winter season is accompanied by the increasing atmospheric thickness in the polar latitudes and the weakening of the midlatitude westerly (i.e., negative phase of the AO) (Kim et al., 2014; Nakamura et al., 2015; Ogawa et al., 2018). The interannual variability of wintertime means the 500 hPa height is almost twice as strong as that of summertime.

In the spring season, the AT over the Middle East shows a significant increase, as in the spring, the high latitude cold

air masses gradually retreat to the north, and the southern regions of the Middle East are escaping the penetration of western winds. Changes in the frequency and intensity of climatic events are an indicator of climate change (Rousta et al., 2018a). As the HGT of 500 hPa streams in the north of the Middle East region are roughly zonal and only when iso-height systems in the northern parts of the Mediterranean and the Middle East are in the path of Western, wind wave can cause the deviation and penetration of the cold weather to the northern and central parts of the Middle East. In the atmospheric maximum specific humidity, which is observed in the wet and warm season, the atmospheric thickness is maximized with the continental air mass prevalence (Rapti, 2005). While the southern regions are completely out of reach of the HGT of the 500-hPa wind waves, they have the highest AT. The optical atmospheric thickness at sea-level lands, such as Denmark, is less than 0.5 annually (Mirhosseini et al., 2018).

In the fall season, the AT has a lower AT than in spring, especially in November and December. Because in the fall season, the western winds and northern latitude streams gradually moved toward low latitudes and, with the influx of cold weather, cause the AT of the Middle East to be reduced. The wind waves from the North Atlantic and the Mediterranean, penetrating to the lower latitudes, cause an advection of cold weather in the western part of the wave in the northern part of the Middle East. While the southern regions of the Middle East in the early fall season, due to the establishment of STHP, have the highest AT. In the atmospheric minimum specific humidity, which is observed in the dry and cold season, the atmospheric thickness is minimized with the prevalence of continental air mass (Rapti, 2005). Therefore, the largest difference in the AT is in the fall season and between the northern and southern parts of the Middle East. The STHPs are retreating and the northern latitude streams are moving toward the southern regions of the Middle East.

The AT peaks in the summer season. Since the main factor controlling the Middle East atmosphere in the summer is the STHP. A core of it is located in the southern regions of Iran and the Persian Gulf basin, and consequently, it causes the increase of the AT in the southern regions of the Middle East. An increase in the atmospheric thickness and mid-tropospheric warming coincides with the vertical structure of a developing tropical low and arguably contributes to the intensification of hurricanes (Wang et al., 2018). Summertime variability in the geopotential height field is weaker and does not exhibit clearly defined teleconnections patterns. Therefore, the deployment of the core of STHPs, on the one hand causes an increase in the AT, and on the other hand, in northern parts of the Middle East, it prevents the penetration of the streams from northern latitudes to the southern parts of the Middle East.

Acknowledgements. This work was supported by Vedurfelagid, Rannis and Rannsoknastofa i vedurfraedi. Iman Rousta is deeply grateful to his supervisor (Haraldur Olafsson, Professor of Atmospheric Sciences, Department of Physics, University of Iceland, Institute for Atmospheric Sciences and Icelandic Meteorological Office (IMO)), for his great support, kind guidance and encouragement.

References

- Alijani, B., 2006: Synoptic Climatology, vol. 1, Tehran-Iran: SAMT press, 1 edn.
- Azizi, G., Mohammadi, H., Karimi, M., Shamsipour, A. A., and Rousta, I., 2015a: *Identification and analysis of the north atlantic blockings*, Int. J. Of Current Life Sci., **5**, 577–581.
- Azizi, G., Mohammadi, H., Karimi, M., Shamsipour, A. A., and Rousta, I., 2015b: *The relationship between the Arctic Oscillation and North Atlantic Blocking Frequency*, Open J Atmos Clim Changes.
- Blackmon, M. L., 1976: *A climatological spectral study of the 500 mb geopotential height of the Northern Hemisphere*, J. Atmos. Sci., **33**, 1607–1623.
- Farajzadeh Asl, M., Ghaemi, H., Zarrin, A., and Azadi, M., 2009: *The Analysis of Spatial Pattern of Subtropical Anticyclones over Asia and Africa*, The Journal of Spatial Planning, **13**, 219–245.
- Ghaemi, H., 2007: *General meteorology*, SAMT Publication, Tehran, Iran, **4**, 570–573.
- Harrell, F., 2015: Regression modeling strategies: with applications to linear models, logistic and ordinal regression, and survival analysis, Springer.
- Houghton, J. T., 1996: Climate change 1995: The science of climate change: contribution of working group I to the second assessment report of the Intergovernmental Panel on Climate Change, vol. 2, Cambridge University Press.
- Iman, R., Faramarz, K. A., Mohsen, S., and Shabnam-Sadat, M. T.: *Assessment of blocking effects on rainfall in northwestern Iran*, 2014.
- Kim, B.-M., Son, S.-W., Min, S.-K., Jeong, J.-H., Kim, S.-J., Zhang, X., Shim, T., and Yoon, J.-H., 2014: *Weakening of the stratospheric polar vortex by Arctic sea-ice loss*, Nat. Commun., **5**, ncomms5646.
- Mirhosseini, M., Rezaniakolaei, A., and Rosendahl, L., 2018: *Numerical Study on Heat Transfer to an Arc Absorber Designed for a Waste Heat Recovery System around a Cement Kiln*, Energies, **11**, 671.
- Nakamura, T., Yamazaki, K., Iwamoto, K., Honda, M., Miyoshi, Y., Ogawa, Y., and Ukita, J., 2015: *A negative phase shift of the winter AO/NAO due to the recent Arctic sea-ice reduction in late autumn*, J. Geophys. Res., **120**, 3209–3227.
- Ogawa, F., Keenlyside, N., Gao, Y., Koenig, T., Yang, S., Suo, L., Wang, T., Gastineau, G., Nakamura, T., Cheung, H. N., et al., 2018: *Evaluating impacts of recent Arctic sea ice loss on the northern hemisphere winter climate change*, Geophys. Res. Lett., **45**, 3255–3263.
- Rapti, A., 2005: *Spectral optical atmospheric thickness dependence on the specific humidity in the presence of continental and maritime air masses*, Atmos. Res., **78**, 13–32.
- Rogers, J. C. and Van Loon, H., 1982: *Spatial variability of sea level pressure and 500 mb height anomalies over the Southern Hemisphere*, Mon. Weather Rev., **110**, 1375–1392.
- Rousta, I.: *Variability of 1000 hpa air temperature and its relation to blocking frequency*, paper presented at the Workshop on Atmospheric Blocking 6-8 April 2016, University of Reading, 2016.
- Rousta, I., Doostkamian, M., Haghghi, E., and Mirzakhani, B., 2016: *Statistical-synoptic analysis of the atmosphere thickness pattern of iran's pervasive frosts*, Climate, **4**, 41.
- Rousta, I., Doostkamian, M., Ólafsson, H., Zhang, H., and Hossein, S., 2018a: *Analyzing the Fluctuations of Atmospheric*

Precipitable Water in Iran During Various Periods Based on the Retrieving Technique of NCEP/NCAR, *Open Atmos. Sci. J.*, **12**, 48–57.

Rousta, I., Javadizadeh, F., Dargahian, F., Ólafsson, H., Shiri-Karimvandi, A., Vahedinejad, S. H., Doostkamian, M., Monroy Vargas, E. R., and Asadolahi, A., 2018b: *Investigation of Vorticity during Prevalent Winter Precipitation in Iran*, *Adv. Meteorol.*, **2018**.

Wang, S. S., Zhao, L., Yoon, J.-H., Klotzbach, P., and Gillies, R. R., 2018: *Quantitative attribution of climate effects on Hurricane Harvey's extreme rainfall in Texas*, *Environ. Res. Lett.*, **13**, 054014.

Zarrin, A., Ghaemi, H., Azadi, M., and Farajzadeh, M., 2010: *The spatial pattern of summertime subtropical anticyclones over Asia and Africa: a climatological review*, *Int. J. Climatol.*, **30**, 159–173.